Two-Dimensional Infrared Spectroscopy of Dimanganese Decacarbonyl and Its Photoproducts: An Ab Initio Study

5 AUTHORS, INCLUDING:

Carlos Baiz
University of Texas at Austin

40 PUBLICATIONS   **406** CITATIONS

Two-Dimensional Infrared Spectroscopy of Dimanganese Decacarbonyl and Its Photoproducts: An Ab Initio Study

Carlos R. Baiz, Porscha L. McRobbie, Nicholas K. Preketes, Kevin J. Kubarych, and Eitan Geva*

Department of Chemistry, University of Michigan, Ann Arbor, Michigan 48109

Received: June 10, 2009; Revised Manuscript Received: July 21, 2009

We present a first-principles study of the 2D carbonyl stretch infrared spectra of dimanganese decacarbonyl, $Mn_2(CO)_{10}$, and its photoproducts, $Mn_2(CO)_9$ and $Mn(CO)_5$. The corresponding multidimensional anharmonic potential energy surfaces are computed via density functional theory up to fourth-order in the normal mode coordinates. The anharmonic shifts are computed using vibrational perturbation theory and benchmarked against results obtained by diagonalizing the vibrational Hamiltonian in the case of $Mn(CO)_5$. The importance of accounting for couplings between the photoactive and photoinactive CO stretches as well as for contributions that arise from fourth-order force constants is demonstrated. The 2D spectra are compared with experiment in the case of $Mn_2(CO)_{10}$. The reasonable agreement between theory and experiment suggests that an approach combining density functional theory with vibrational perturbation theory can provide a useful route for computing 2D infrared spectra, particularly in cases where direct diagonalization of the vibrational Hamiltonian is not feasible.

I. Introduction

Over the past decade, two-dimensional infrared (2DIR) spectroscopy has established itself as a powerful probe of molecular structure and dynamics.[1–3] Structural information is typically obtained from the spectral peak positions and intensities, whereas dynamical information can be obtained from the lineshapes and the dependence of the 2D spectra on the waiting time between the pump and the probe pulses. The recent introduction of nonequilibrium 2DIR spectroscopy has also made it possible to use 2DIR spectroscopy to probe nonequilibrium dynamics triggered by electronic photoexcitation.[4–6]

Metal−carbonyl complexes have proven to be useful benchmark systems for 2DIR spectroscopy.[7–11] In particular, the measurement and analysis of the 2DIR spectrum of the coupled symmetrical and antisymmetrical carbonyl stretch modes in $Rh(CO)_2C_5H_7O_2$ (RDC) have led to important insight into how anharmonicity, mode−mode coupling, the tensorial nature of optical response, and rotational relaxation affect 2DIR spectra.[12–14] The interpretation of the spectra originally relied on simple models with empirically fitted parameters. Such an intuitive approach is tractable in a system like RDC because it can be modeled in terms of only two coupled anharmonic modes and using a relatively small number of empirical parameters. However, the empirical nature of the models employed and the fact that they relied on uncontrollable approximations made it desirable to develop a more general ab initio modeling approach. Indeed, an ab initio approach to modeling 2DIR spectra, which relies on input obtained from electronic structure calculations, has been recently demonstrated with considerable success on several polyatomic systems, including RDC.[11,15–21] More specifically, Moran and coworkers[11] have recently produced a 2DIR spectrum of RDC by computing the 2D anharmonic potential energy surface in terms of the carbonyl stretch coordinates up to fourth-order via DFT and numerically diagonalizing the corresponding Hamiltonian. The computed 2DIR spectrum was found to be in reasonable agreement with the experimental spectrum obtained by Tokmakoff and coworkers.[7,10] Most importantly, their work has revealed that fourth-order force constants can have a significant effect on the spectral features, even though the experimental 2DIR spectrum was originally fit to a model that ignored them. Whereas the empirical and theoretical approaches mentioned above appear to be adequate for a small system like RDC, they become impractical as the size of the system is increased. More specifically, in a system like $Mn_2(CO)_{10}$, one would need to employ hundreds of fitting parameters, and the resulting parameter set is not likely to be unique. It should also be noted that the effective dimensionality of the system may not be determined by the number of IR active modes because IR-inactive modes may also affect the spectra if they are strongly coupled to the IR-active modes.

In this article, we present an ab initio approach for calculating 2DIR spectra of the carbonyl stretch modes in $Mn_2(CO)_{10}$ and its photoproducts $Mn(CO)_5$ and $Mn_2(CO)_9$. (See Figure 1.) The choice of system is motivated by the availability of equilibrium 2DIR spectra for $Mn_2(CO)_{10}$ and the difficulty of measuring the equilibrium 2DIR spectra of its relatively unstable photoproducts. It should be noted that with 10 (four active and six inactive), 5 (three active and two inactive), and 9 (all active) highly delocalized CO stretch modes in $Mn_2(CO)_{10}$, $Mn(CO)_5$, and $Mn_2(CO)_9$, respectively, this system is considerably more challenging than RDC (which only involves two active modes).

The UV photolysis of $Mn_2(CO)_{10}$ has been extensively studied, both theoretically[22–29] and experimentally, in the gas phase,[30–32] liquid solution,[33–39] and low-temperature matrices.[40–43] It is well established that the two primary photochemical events that take place are: (1) homolytic cleavage of the Mn−Mn bond to form the square pyramidal $Mn(CO)_5$ and (2) CO ligand dissociation to form $Mn_2(CO)_9$, whose structure involves a bridging carbonyl across the Mn−Mn bond. The fact that $Mn_2(CO)_{10}$, $Mn(CO)_5$, and $Mn_2(CO)_9$ have distinctly different IR spectra has turned time-resolved IR spectroscopy into a powerful tool for studying photodissociation in this system.[37]

* Corresponding author. Email: eitan@umich.edu.

9618 *J. Phys. Chem. A, Vol. 113, No. 35, 2009*

Baiz et al.
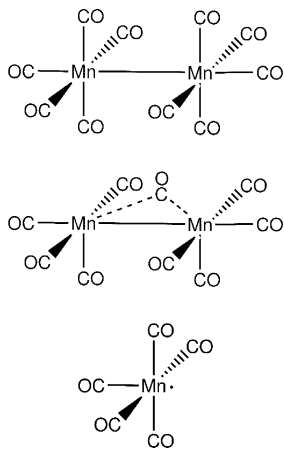
Figure 1. Chemical structure of dimanganese decacarbonyl [Mn$_2$(CO)$_{10}$] and two photoproducts, dimanganese nonacarbonyl [Mn$_2$(CO)$_9$] and manganese pentacarbonyl [Mn(CO)$_5$].

The photodissociation reaction is believed to involve a singlet−singlet $\sigma_{Mn-Mn} \rightarrow \sigma^*_{Mn-Mn}$ and $3d_{Mn} \rightarrow \sigma^*_{Mn-Mn}$ photoexcitations, followed by intersystem crossing to the corresponding dissociative triplet states.[28] The calculation of the equilibrium 2DIR spectra of Mn$_2$(CO)$_{10}$, Mn(CO)$_5$, and Mn$_2$(CO)$_9$ therefore constitutes an important first step toward understanding the spectral signature of the photodissociation process as measured via optical-pump/2DIR-probe techniques. The main challenges involved in computing the 2DIR spectra of Mn$_2$(CO)$_{10}$ and its photoproducts include: (1) the small spectral shifts that require high accuracy to be resolved; (2) the relatively large number of CO stretches; (3) the fact that the state-to-state transition dipole moments are oriented along different directions, which makes it necessary to account for the tensorial nature of optical response; and (4) the relatively strong coupling between the active and inactive CO stretch modes.

The structure of the remainder of this article is as follows. In Sections II and III, we describe the methods used for computing the anharmonic potential energy surface and obtaining the vibrational energy levels, either by diagonalizing the Hamiltonian (when possible) or via vibrational perturbation theory. The calculated 2DIR spectra for Mn$_2$(CO)$_{10}$ and its photoproducts are presented and analyzed in Section IV. The main results are summarized in Section V.

II. Anharmonic Vibrational Hamiltonian

The anharmonic Hamiltonian up to fourth-order in terms of the normal mode coordinates is given by

$$H = \frac{1}{2}\sum_i \phi_{ii}(q_i^2 + p_i^2) + \frac{1}{6}\sum_{ijk}\phi_{ijk}q_iq_jq_k + \frac{1}{24}\sum_{ijkk}\phi_{ijkk}q_iq_jq_k^2 \tag{1}$$

Third-order force constants, ϕ_{ijk}, and semidiagonal fourth-order force constants, ϕ_{ijkk}, were calculated in terms of the normal-mode coordinates via a finite displacement method.[44,45] Off-diagonal fourth-order force constants of the type ϕ_{ijkl} have been observed to lead to very small shifts of the energy levels (∼1 cm^{-1}) and are therefore neglected.[46] More specifically, the second derivatives of the potential energy with respect to the normal mode coordinates $\phi_{ij} = \partial^2 U/\partial q_i \partial q_j$ were calculated at the equilibrium geometry as well as at geometries slightly displaced relative to it. We obtained the displaced configurations by shifting the atoms relative to their equilibrium positions along

all 3N-6 normal-mode coordinates in the positive and negative directions. For a given displacement Δq_k along the kth mode coordinate, the third-order force constant is given by

$$\phi_{ijk} = \left[\frac{\partial^3 U}{\partial q_i \partial q_j \partial q_k}\right]_{\mathbf{q}=0} = \frac{\phi_{ij}^+ - \phi_{ij}^-}{2\Delta q_k} \tag{2}$$

where ϕ_{ij}^+ and ϕ_{ij}^- represent the second-order force constants at the positively and negatively displaced geometries, respectively. Similarly, the semidiagonal fourth-order force constants are given by

$$\phi_{ijkk} = \left[\frac{\partial^4 U}{\partial q_i \partial q_j \partial q_k^2}\right]_{\mathbf{q}=0} = \frac{\phi_{ij}^+ + \phi_{ij}^- - 2\phi_{ij}^0}{2(\Delta q_k)^2} \tag{3}$$

where $\phi_{ij}^0 \equiv \phi_{ii}^0\delta(i,j)$ is the second-order constant at the equilibrium geometry. The most straightforward approach to obtaining the stationary wave functions and energy levels of the Hamiltonian in eq 1 associated with the fundamental and overtone transitions is by direct diagonalizion. This approach works well for a system where the number of modes of interest is small, such as RDC. However, because the size of the Hamiltonian matrix grows exponentially with respect to the number of modes, direct diagonalization becomes unfeasible for a system with more than a few modes. One way of avoiding direct diagonalization is by using second-order vibrational perturbation theory (VPT2), which is based on using the harmonic stationary states and energy levels as the zero-order approximation and assuming that the anharmonicities can be treated as small perturbations.[47−50] Assuming that the harmonic transition dipole moments are sufficiently accurate, one can combine them with the anharmonic transition frequencies obtained via VPT2, thereby giving rise to a feasible route for computing spectra of systems like Mn$_2$(CO)$_{10}$ that have a large number of modes.

III. Ab Initio Methods

Molecular geometries were optimized with DFT. The choices of density functional and basis sets were guided by previously reported calculations of anharmonic vibrational frequencies in small molecules.[50−52] The results reported in the present study were obtained using Becke's 1988 exchange functional[53] and Perdew's 1986 correlation functional[54] (BP86) with a LanL2DZ pseudopotential[55] basis on manganese and 6-31G(d) basis on the carbon and oxygen atoms. This particular choice of density functionals and basis sets was found to give the best agreement with experiment such that the computed frequencies are within ∼1% of the experimental values. (See Table 1.) We have also found that a tight optimization threshold was required to obtain reliable third- and fourth-order force constants. Therefore, optimization convergences needed to be set to 10^{-6} hartrees/bohr of maximum gradient, and the SCF convergence needed to be set to 10^{-10} hartrees. Frequency analyses were carried out at the equilibrium and 6N-11 displaced geometries. All Cartesian geometry optimizations and second-derivative matrix computations were carried out using Q-Chem 3.1.[56]

The displacement along the normal modes, Δq, was set to 0.03 after tests indicated that the force constants are independent of the displacement for values between 0.01 and 0.03. It should be noted that the displacement should be small enough so that higher-order terms do not significantly contribute yet contribute

TABLE 1: Experimental, Harmonic, And Anharmonic (via VPT2) Fundamental Transition Frequencies for Mn$_2$(CO)$_{10}$ and Its Photoproducts (in inverse centimeters)

	Mn$_2$(CO)$_{10}$			Mn$_2$(CO)$_9$			Mn(CO)$_5$		
mode	exptl	Harmonic	VPT2	exptl	harmonic	VPT2	exptl	harmonic	VPT2
1	1981[a]	1972.5	1912.2	1760[c]	1786.9	1752.9		1981.1	1952.5
2	1981[a]	1972.5	1909.9	1966[c]	1968.8	1934.3	1982[d]	1985.6	1956.9
3	1983[b]	1980.6	1964.1		1979.2	1949.2	1982[d]	1985.6	1956.1
4	1997[a]	1990.7	1985.5	1994[c]	1987.5	1839.7		2000.5	1970.6
5	2014[b]	2004.8	1939.6	2006[c]	1994.5	1984.1		2080.0	2047.9
6	2014[b]	2004.9	1937.4		2007.6	1974.8			
7	2024[a]	2005.6	1960.3	2020[c]	2008.4	1979.0			
8	2024[a]	2008.6	1921.4	2058[c]	2040.1	1993.8			
9	2044[b]	2035.6	1993.6		2085.6	2044.3			
10	2116[a]	2097.0	2039.4						

[a] Experimental frequencies obtained from Raman scattering in light petroleum.[60] [b] Experimental frequencies obtained from FTIR in *n*-hexane. [c] Experimental frequencies obtained from transient absorption in cyclohexane.[30] [d] Experimental frequencies obtained from transient absorption in cyclohexane.[37]

enough so as to minimize numerical errors arising from the SCF procedure. It is also important to emphasize that although the harmonic frequencies may contain systematic errors that arise from using DFT, it is reasonable to expect these errors to be the same at the equilibrium and displaced configurations and therefore to cancel out and yield accurate third- and fourth-order force constants.[57]

Anharmonic energy levels were computed via the standard VPT2 method using the full set (third- and fourth-order) of force constants. The VPT2 calculation was also repeated using subsets of the force constants to investigate the importance of contributions from fourth-order force constants relative to those from third-order constants and the importance of contributions from photoactive modes relative to photoinactive modes. It should be pointed out that the VPT2 anharmonic method is currently implemented in many popular electronic structure packages. However, these packages will only perform the perturbation using the full set of force constants. Therefore, applying VPT2 to models involving subsets of the force constants and modes requires us to write our own code.

For the sake of benchmarking, it was desirable to compare the VPT2 results with results obtained via direct diagonalization. To this end, we have computed anharmonic energy levels and wave functions for all five CO stretches of Mn(CO)$_5$ obtained using the full vibrational Hamiltonian. Using this procedure, it was necessary to increase the size of the harmonic basis until convergence of the anharmonic energy levels was reached. For example, in the case of Mn(CO)$_5$, the number of basis functions per mode needed to converge the first- and second-excited energy levels is seven; with a total of $7^5 = 16\,807$ basis functions. To minimize memory requirements, the Hamiltonian was stored as a sparse matrix and the lowest 30 eigenvalues and eigenvectors were computed iteratively via the Arnoldi method as implemented in the ARPACK subroutine library.[58] Note that this iterative method is equivalent to numerically diagonalizing the Hamiltonian matrix, and thus in the following section, we use both terms interchangeably.

IV. Results and Discussion

In Table 1, we present a comparison of the harmonic and VPT2-based anharmonic fundamental frequencies with the corresponding experimental values for Mn$_2$(CO)$_{10}$, Mn (CO)$_5$, and Mn$_2$(CO)$_9$. The harmonic frequencies are found to be in good agreement with the experimental values for all three molecules. The anharmonic frequencies are shifted down by ~10−60 cm^{-1} below the experimental values and do not

preserve the relative ordering of the frequencies. This behavior of DFT/VPT2 has been previously observed in other molecules[50,59] and can be attributed to Fermi or other types of resonances between the carbonyl modes and low-frequency modes or inaccuracies brought about by the use of DFT as well as the fact that such effects as solvent shifts have not been accounted for. In the case of our metal carbonyl molecules, the CO modes are isolated in frequency, and the coupling to the lower frequency modes is small; therefore, we avoid errors arising from Fermi resonances by performing the perturbation on the CO modes only. This approach, however, may not work in other systems where the modes may be more highly coupled and not as well isolated in frequency. Nevertheless, as we will see below, the actual values of the anharmonic shifts, rather than the absolute value of the fundamental frequencies, are still reproduced rather well with this approach when using the full set of force constants. One may, therefore, adopt a strategy that combines the harmonic fundamental frequencies, which happen to be in excellent agreement with experiment, with anharmonic shifts obtained via VPT2.

In Table 2, we report the diagonal anharmonic shifts obtained for Mn$_2$(CO)$_{10}$ via VPT2. The entries in the second and third columns of this table correspond to the anharmonic shifts obtained by applying VPT2 to a model that includes all 3N-6 vibrational modes, using either only the third-order force constants or the third-order and fourth-order force constants, respectively. The fourth-order force constants are seen to affect the anharmonic shifts significantly. Similar results obtained for RDC by Moran et al.[11] using a full diagonalization of a two-mode Hamiltonian have also demonstrated the importance of including higher-than-third-order force constants. Therefore, our results reinforce the view that the fact that an experimental 2DIR spectrum can be fitted to a model that only accounts for third-order anharmonicities does not exclude the possibility that higher-order force constants are important, particularly in cases where ab initio calculations suggest that this is the case.[7]

The fourth column of Table 2 shows the anharmonic shifts obtained by applying VPT2 to a model that includes only the ten CO stretch modes. The similarity between those results and the results obtained for an all-mode model (second column) indicates that the CO stretch modes are essentially decoupled from the other vibrational modes of the complex. This is not surprising because the CO stretch modes are largely isolated in frequency so that coupling to other lower frequency modes is expected to be weak compared with the coupling among these CO stretch modes. The fifth column of Table 2 shows the

TABLE 2: Diagonal Anharmonic Shifts, $\Delta = \omega_{0\to1} - \omega_{1\to2}$ for Mn₂(CO)₁₀, in inverse centimeters, As Obtained Using VPT2[a]

	all modes		CO modes	IR active CO modes	
mode	3rd and 4th order	3rd order only	3rd and 4th order	3rd and 4th order	exptl
1	5.2	10.2	4.3		
2	5.3	10.2	4.3		
3	6.5	12.8	5.4	−6.3	8.3
4	9.7	19.1	8.0		
5	5.5	10.3	4.5	−4.7	6.5
6	5.5	10.3	4.5	−4.7	6.5
7	3.9	7.4	3.0		
8	4.6	7.6	3.7		
9	3.2	5.3	2.5	−2.1	4.4
10	3.4	5.0	2.6		

[a] A positive anharmonic shift means that the excited-state absorption peak appears at a lower frequency than the ground-state bleach. A comparison is made for frequencies where the perturbation includes all modes (columns two and three), only CO modes (column four), and only the IR active CO modes (column five). The second and third columns also show the anharmonicities obtained by using third- and fourth-order force constants and only the third-order force constants, respectively. Experimental values are obtained from fits to transient absorption spectra.

anharmonic shifts obtained by applying VPT2 to a model that includes only the four photoactive CO stretch modes. A comparison to the results in the fourth column clearly reveals that neglecting the coupling between the photoactive and photoinactive CO stretch modes leads to qualitatively incorrect results. More specifically, the sign of the anharmonic shifts is reversed so that the overtone frequencies become larger than the fundamental frequencies.

The comparison with the experimental results (column six) reveals that a minimal model must include at least all ten CO stretches, whether photoactive or not, and account for anhar-
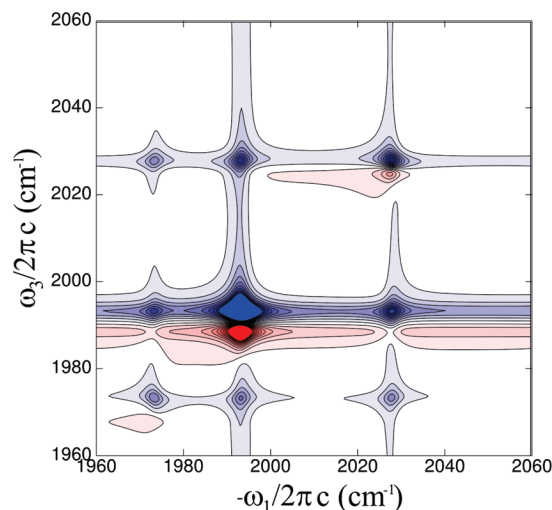
Figure 3. Theoretical absorptive 2DIR spectrum of Mn₂(CO)₁₀ at zero waiting time computed in the zzzz polarization geometry. Red contours correspond to positive peaks, whereas negative contours represent negative peaks. Contours larger than 20% of the maximum amplitude are omitted.

monic force constants at least up to fourth order. It is important to note that with such small anharmonic shifts, one cannot expect quantitative agreement with experiment. However, the fact that the trends and orders of magnitude are in reasonable agreement with experiment is quite encouraging.

The experimental 2DIR spectrum of Mn₂(CO)₁₀ has been analyzed in detail in a previous paper.[61] In brief, the spectrum shows three main peaks along the diagonal with cross peaks between all transitions. The three peaks correspond to four transitions at 1983, 2014, 2014, and 2045 cm⁻¹ with B_2, E_1, E_1, and B_2 symmetry, respectively. The transition dipole moments associated with the B modes are parallel to the Mn−Mn axis, whereas those associated with the degenerate
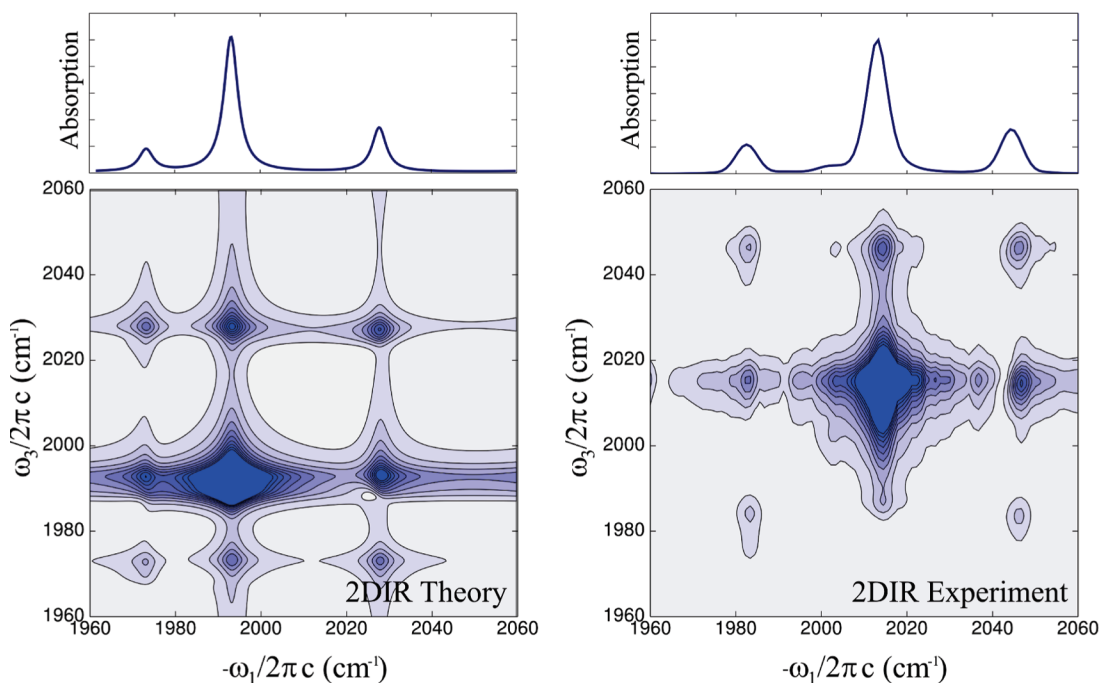
Figure 2. (left) Theoretical absorption (upper traces) and absolute-value rephasing 2DIR spectra of Mn₂(CO)₁₀ using the VPT2 frequencies (Table 2, column 4) and diagonal anharmonicities. No empirical frequency scaling is used. (right) Experimental absorption and Fourier-transform absolute-value rephasing 2DIR spectra of Mn₂(CO)₁₀ in cyclohexane measured in the zzzz polarization geometry at zero waiting time. Contours larger than 20% of the total amplitude are omitted for clarity.

2DIR Spectroscopy of Mn$_2$(CO)$_{10}$ and Its Photoproducts

J. Phys. Chem. A, Vol. 113, No. 35, 2009 **9621**

TABLE 3: Comparison of the Mn(CO)$_5$ Energy Levels Obtained by Computation of the Hamiltonian Eigenvalues (Full Ham.) and Those Obtained by VPT2^a

Mn(CO)$_5$ - All CO Modes				
State (Harmonic)	Full Ham.		VPT2	
1 (1981.1)	1956.9		1952.5	
2 (1985.6)	1952.4		1956.9	
3 (1985.6)	1952.4		1956.1	
4 (2000.5)	1966.0		1970.6	
5 (2080.0)	2045.5		2047.9	
Overtones		Δ		Δ
11	3893.2	20.6	3884.6	20.4
22	3880.1	24.6	3905.8	8.0
33	3880.1	24.6	3904.2	8.0
44	3933.2	−1.1	3935.3	6.0
55	4084.0	7.0	4090.5	5.3
Comb.				
32	3876.6	28.2	3904.1	8.8
24	3883.4	35.0	3915.0	12.5
31	3912.9	−3.6	3907.7	0.9
41	3923.6	−0.6	3922.2	1.0
53	3987.3	10.6	3992.5	11.5
51	3994.2	8.3	3993.7	6.7
Mn(CO)$_5$ - IR Active Modes Only				
State	Full Ham.		VPT2	
2	1996.3		1999.8	
3	1996.3		1999.8	
Overtones		Δ		Δ
22	4001.6	−8.9	4008.8	−9.2
33	4003.1	−10.4	4008.7	−9.1
Comb.				
23	3994.2	−1.5	4009.6	−10.0

^{a} Fundamentals, overtones, and a few selected combination (Comb.) bands are shown. The anharmonic shifts (Δ = $\omega_{0\rightarrow1}$ − $\omega_{1\rightarrow2}$) correspond to the difference between two-quantum transitions and twice the fundamental transitions. To simplify notation, we denote the state by the number of excitations within each corresponding mode $|n_1n_2n_3n_4n_5\rangle \equiv n_i$ for singly excited states and $||n_1n_2n_3n_4n_5\rangle \equiv n_in_j$ for doubly excited states ($i = j$ for overtones, $i \neq j$ for combination). For example, 1 = $|10000\rangle$, 11 = $|20000\rangle$, 34 = $|00110\rangle$, and so on. The information contained in the upper portion of this table is shown graphically as energy level diagrams in Figure 4.

E-modes are oriented perpendicular to each other and to the Mn−Mn axis. The experimental techniques used to measure multidimensional IR spectra have been thoroughly documented elsewhere and are therefore not discussed here.[9,61−63]

The absolute value rephrasing 2DIR spectra in the zzzz polarization geometry are compared with the corresponding experimental spectra in Figure 2. The spectra were calculated using the VPT2-based anharmonic frequencies (fundamentals, overtones, and combination states) computed using all third- and fourth-order force constants involving all ten CO stretch modes. The harmonic transition dipole moments were used because excellent agreement is observed when comparing the computed and experimental linear absorption spectra. Optical response functions were calculated via SPECTRON,[64] within the framework of Redfield theory, using a phenomenological homogeneous width (Γ = 2 cm^{-1}). The general qualitative agreement with experiment is satisfactory, considering the fact that no scaling factors were used. The two spectra show that in the case of the absolute value rephrasing 2DIR spectrum the anharmonic peaks are buried underneath the fundamental peaks.

The calculated absorptive 2DIR spectrum of Mn$_2$(CO)$_{10}$ is shown in Figure 3. In this case, it is predicted that the off-
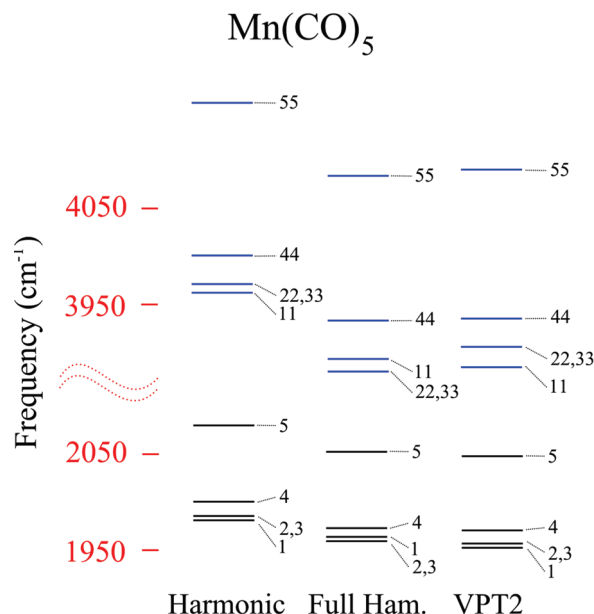
Figure 4. Comparison between the three methods for the one- and two-quanta energy levels of [Mn(CO)$_5$]. The energy levels represented in this diagram are also shown in Table 3.

diagonal anharmonic peaks, which correspond to Liouiville paths that involve two-quantum combination states, would be resolved. It should be noted that the additional peak present in the experimental absorption and absolute value rephrasing 2DIR spectra at 2002 cm^{-1} is due to natural ^{13}C isotope present in the molecule.[62] A single ^{13}C substitution on an axial carbonyl splits the 2013 cm^{-1} mode into two modes centered at 2013 and 2002 cm^{-1}. Therefore, cross peaks are observed in the 2DIR spectrum between these two diagonal transitions. Finally, Figure 2 shows that the computed oscillator strengths are also in good agreement with experiment. [Note added in proof: A recently-measured absorptive 2DIR spectrum of Mn$_2$(CO)$_{10}$ shows excellent qualitative agreement with the theoretical prediction.]

Next, we compare the VPT2 results with results obtained via a direct diagonalization in the case of Mn(CO)$_5$. (See Table 3.) Because of the computational expense involved in generating, storing, and diagonalizing the vibrational Hamiltonian, it was not possible to perform a similar comparison in the cases of Mn$_2$(CO)$_{10}$ or Mn$_2$(CO)$_9$. The agreement between the frequencies obtained with VPT2 and numerical diagonalization validates the perturbation treatment. The second part of Table 3 shows the same comparison within a model that includes only the two degenerate photoactive CO stretch modes. Once again, the VPT2 and numerical diagonalization energy levels are observed to be in excellent agreement, both yielding negative anharmonic shifts. As discussed above, these negative anharmonicities are not qualitatively correct compared with experiment; however, the results show that VPT2 is still able to produce reliable frequencies in comparison with numerical diagonalization using a reduced set of force constants. In addition, these observations once again underscore the fact that all strongly coupled modes, either photoactive or not, must be explicitly included to reproduce the experimental spectra.

Table 4 shows the fundamental and diagonal overtone transition frequencies of the CO stretches in Mn$_2$(CO)$_9$, as obtained via VPT2. In the second and third column, we show the results obtained based on a model that included all 3N-6 vibrational modes of the molecule, whereas in the fourth and fifth columns, we show results obtained on the basis of a model that only included the 9 CO stretch modes. Interestingly, in this

TABLE 4: VTP2 Frequencies for $Mn_2(CO)_9$ in inverse centimeters along with Overtones and Anharmonic Shifts ($\Delta = 2\omega_{0\rightarrow1} - \omega_{1\rightarrow2}$) Computed Using the Full Set of Force Constants (All Modes) and a Reduced Set of Force Constants Involving Only the Carbonyl Stretching Modes

mode (harmonic)	$Mn_2(CO)_9$ - VPT2 all modes			$Mn_2(CO)_9$ - VPT2 CO modes only		
	fundamental	overtone	δ	fundamental	overtone	Δ
1 (1786.9)	1752.9	3478.6	27.2	1769.8	3520.9	18.6
2 (1934.2)	1934.3	3857.0	11.6	1949.2	3888.9	9.5
3 (1979.2)	1949.2	3892.0	6.4	1957.2	3909.0	5.4
4 (1987.5)	1839.7	3665.2	14.2	1953.8	3895.9	11.8
5 (1994.5)	1984.1	3959.3	8.9	1977.8	3948.5	7.1
6 (2007.6)	1974.8	3943.8	5.9	1987.6	3970.4	4.8
7 (2008.4)	1979.0	3951.6	6.5	1986.4	3967.5	5.3
8 (2040.1)	1993.8	3983.8	3.8	2018.9	4034.8	2.9
9 (2085.6)	2044.3	4085.0	3.6	2064.4	4126.0	2.8

case, the results of the two calculations are considerably different. In particular, the large deviation by more than 100 cm^{-1} in the case of mode 4 is indicative of significant coupling between this CO stretch and lower frequency modes. The table also shows that the anharmonic shift of mode 1 (27.2 cm^{-1}) is larger than the rest. This can be attributed to the fact that this mode corresponds to the stretching of the bridging carbonyl, which is expected to be more anharmonic because of the fact that it is simultaneously bonded to both metal centers.

Theoretical 1D and 2D IR spectra of $Mn_2(CO)_9$ (zzzz polarization geometry) are shown in Figure 5. At present, only a transient absorption spectrum of this species is available in the literature.[34] The harmonic and VPT2 frequencies for $Mn_2(CO)_9$, shown in Table 1, are in reasonable agreement with the experimental values. The measurement of nonequilibrium 2DIR spectra of $Mn_2(CO)_9$ is currently underway in our laboratory. Given the good agreement between experiment and theory in the case of $Mn_2(CO)_{10}$, we expect that the computed spectrum for $Mn_2(CO)_9$ also provides a reliable depiction of the actual spectra of this species.
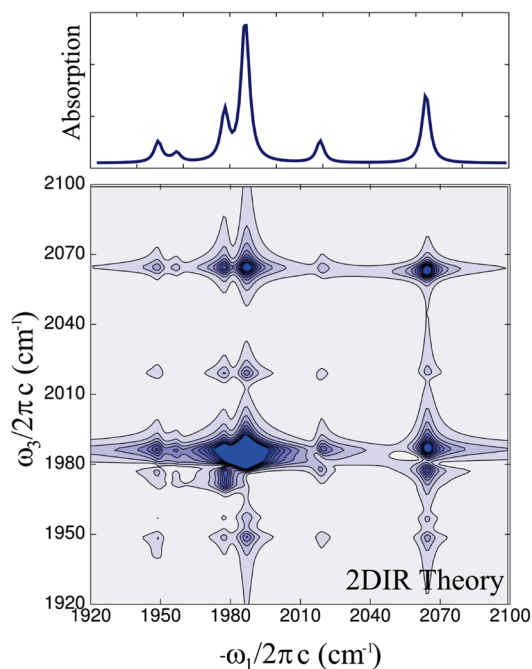
Figure 5. Theoretical absorption (upper trace) and absolute-value rephasing 2DIR spectra of $Mn_2(CO)_9$ at zero waiting time computed in the zzzz polarization geometry using the VPT2 anharmonic frequencies and harmonic transition dipole moments. Contours larger than 20% of the total amplitude are omitted for clarity.

V. Conclusions and Summary

In this study, we have explored the use of a methodology that combines ab initio DFT (BP86/LanL2DZ) calculations with VPT2 to compute the experimentally relevant 1D and 2D spectra of $Mn_2(CO)_{10}$ and its photoproducts $Mn(CO)_5$ and $Mn_2(CO)_9$. We have demonstrated that predictive self-consistent treatment must account for higher-than-third-order anharmonic force constants and include all highly coupled modes, regardless of whether they are photoactive. In the case of metal carbonyls, this modeling implied accounting for at least fourth-order anharmonic force constants and including at least all CO stretch modes. We have also demonstrated the accuracy of VPT2 by benchmarking it against results obtained via direct diagonalization in the case of $Mn(CO)_5$.

Further motivation for future modeling of $Mn(CO)_5$ arises from recent nonequilibrium 2DIR experiments, which have provided evidence of solute−solvent complexes.[39] Solvent complexation may distort the molecular geometry causing the dark modes to become active; an effect that would be captured by the modeling methods presented here. These effects may be captured by using continuum solvent models in the electronic structure computations or by explicitly adding a small number of nearby solvent molecules to the molecule. In addition, cross peaks in 2DIR spectra are sensitive to vibrational energy transfer among the vibrational modes, which in turn is directly mediated by through-bond anharmonic coupling and spatial overlap of the wave functions.[65,66] Because energy transfer may likely involve IR inactive modes, modeling of these energy relaxation measurements would require knowledge of all coupling constants.

Finally, it should be noted that although fourth-order force constants impact 2DIR spectra, higher-order nonlinear spectroscopies are expected to be even more sensitive to it. In this context, it is interesting to note that several fifth-order infrared experiments have been reported recently, under either equilibrium[67] or nonequilibrium conditions.[63,68] Because peak assignments are likely to be even more challenging in this case, one expects that electronic structure methods of the type described herein will prove to be useful for the interpretation of these experiments.

2DIR Spectroscopy of Mn$_2$(CO)$_{10}$ and Its Photoproducts

J. Phys. Chem. A, Vol. 113, No. 35, 2009 **9623**

References and Notes

(1) Cho, M. *Chem. Rev.* **2008**, *108*, 1331–1418.

(2) Zheng, J.; Kwak, K.; Fayer, M. *Acc. Chem. Res.* **2007**, *40*, 75–83.

(3) Mukamel, S. *Annu. Rev. Phys. Chem.* **2000**, *51*, 691–729.

(4) Hamm, P.; Helbing, J.; Bredenbeck, J. *Annu. Rev. Phys. Chem.* **2008**, *59*, 291–317.

(5) Kolano, C.; Helbing, J.; Kozinski, M.; Sander, W.; Hamm, P. *Nature* **2006**, *444*, 469–472.

(6) Andresen, E. R.; Hamm, P. *J. Phys. Chem. B* **2009**, *113*, 6520–6527.

(7) Khalil, M.; Demirdoven, N.; Tokmakoff, A. *J. Phys. Chem. A* **2003**, *107*, 5258–5279.

(8) Merchant, K. A.; Thompson, D. E.; Fayer, M. D. *Phys. Rev. Lett.* **2001**, *86*, 3899.

(9) Nee, M. J.; McCanne, R.; Kubarych, K. J.; Joffre, M. *Opt. Lett.* **2007**, *32*, 713–715.

(10) Golonzka, O.; Khalil, M.; Demirdoven, N.; Tokmakoff, A. *J. Chem. Phys.* **2001**, *115*, 10814–10828.

(11) Moran, A. M.; Dreyer, J.; Mukamel, S. *J. Chem. Phys.* **2003**, *118*, 1347–1355.

(12) Sung, J.; Silbey, R. J. *J. Chem. Phys.* **2001**, *115*, 9266–9287.

(13) Tokmakoff, A. *J. Chem. Phys.* **1996**, *105*, 1–12.

(14) Hochstrasser, R. M. *Chem. Phys.* **2001**, *266*, 273–284.

(15) Heyne, K.; Huse, N.; Dreyer, J.; Nibbering, E. T. J.; Elsaesser, T.; Mukamel, S. *J. Chem. Phys.* **2004**, *121*, 902–902.

(16) Hayashi, T.; Mukamel, S. *J. Phys. Chem. A* **2003**, *107*, 9113–9131.

(17) Hayashi, T.; Jansen, T. l. C.; Zhuang, W.; Mukamel, S. *J. Phys. Chem. A* **2005**, *109*, 64–82.

(18) Dreyer, J. *Int. J. Quantum Chem.* **2005**, *104*, 782–793.

(19) Park, K.; Cho, M.; Hahn, S.; Kim, D. *J. Chem. Phys.* **1999**, *111*, 4131–4139.

(20) Wang, J. *J. Phys. Chem. B* **2007**, *111*, 9193–9196.

(21) Kwak, K.; Cha, S.; Cho, M.; Wright, J. C. *J. Chem. Phys.* **2002**, *117*, 5675–5687.

(22) Brown, D. A.; Chambers, W. J.; Fitzpatrick, N. J.; Rawlinson, R. M. *J. Chem. Soc. A* **1971**, 720–725.

(23) Elian, M.; Hoffmann, R. *Inorg. Chem.* **1975**, *14*, 1058–1076.

(24) Nakatsuji, H.; Hada, M.; Kawashima, A. *Inorg. Chem.* **1992**, *31*, 1740–1744.

(25) Folga, E.; Ziegler, T. *J. Am. Chem. Soc.* **1993**, *115*, 5169–5176.

(26) Rosa, A.; Ricciardi, G.; Baerends, E. J.; Stufkens, D. J. *Inorg. Chem.* **1995**, *34*, 3425–3432.

(27) van Gisbergen, S. J. A.; Groeneveld, J. A.; Rosa, A.; Snijders, J. G.; Baerends, E. J. *J. Phys. Chem. A* **1999**, *103*, 6835–6844.

(28) Kuhn, O.; Hachey, M. R. D.; Rohmer, M. M.; Daniel, C. *Chem. Phys. Lett.* **2000**, *322*, 199–206.

(29) Daniel, C. *Coord. Chem. Rev.* **2003**, *238*, 143–166.

(30) Seder, T. A.; Church, S. P.; Weitz, E. *J. Am. Chem. Soc.* **1986**, *108*, 7518–7524.

(31) Marquez, A.; Sanz, J. F.; Gelize, M.; Dargelos, A. *J. Organomet. Chem.* **1992**, *434*, 235–240.

(32) Kim, S. K.; Pedersen, S.; Zewail, A. H. *Chem. Phys. Lett.* **1995**, *233*, 500–508.

(33) Rothberg, L. J.; Cooper, N. J.; Peters, K. S.; Vaida, V. *J. Am. Chem. Soc.* **1982**, *104*, 3536–3537.

(34) Church, S. P.; Hermann, H.; Grevels, F. W.; Schaffner, K. *J. Chem. Soc., Chem. Commun.* **1984**, 785–786.

(35) Zhang, J. Z.; Harris, C. B. *J. Chem. Phys.* **1991**, *95*, 4024–4032.

(36) Waldman, A.; Ruhman, S.; Shaik, S.; Sastry, G. N. *Chem. Phys. Lett.* **1994**, *230*, 110–116.

(37) Steinhurst, D. A.; Baronavski, A. P.; Owrutsky, J. C. *Chem. Phys. Lett.* **2002**, *361*, 513–519.

(38) Owrutsky, J.; Baronavski, A. *J. Chem. Phys.* **1996**, *105*, 9864–9873.

(39) Baiz, C. R.; McCanne, R.; Nee, M. J.; Kubarych, K. J. *J. Phys. Chem. A* **2009**, *113*, 8907–8916.

(40) Dunkin, I. R.; Harter, P.; Shields, C. J. *J. Am. Chem. Soc.* **1984**, *106*, 7248–7249.

(41) Hepp, A. F.; Wrighton, M. S. *J. Am. Chem. Soc.* **1983**, *105*, 5934–5935.

(42) Martin, M.; Rees, B.; Mitschler, A. *Acta Crystallogr., Sect. B: Struct. Sci.* **1982**, *38*, 6–15.

(43) Church, S. P.; Poliakoff, M.; Timney, J. A.; Turner, J. J. *J. Am. Chem. Soc.* **1981**, *103*, 7515–7520.

(44) Schneider, W.; Thiel, W. *Chem. Phys. Lett.* **1989**, *157*, 367–373.

(45) Dressler, S.; Thiel, W. *Chem. Phys. Lett.* **1997**, *273*, 71–78.

(46) Lin, C.; Gilbert, A.; Gill, P. *Theor. Chem. Acc.* **2008**, *120*, 23–35.

(47) Califano, S. *Vibrational States*; John Wiley and Sons: London, 1976.

(48) Barone, V. *J. Chem. Phys.* **2005**, *122*, 014108.

(49) Barone, V. *J. Chem. Phys.* **2004**, *120*, 3059–3065.

(50) Neugebauer, J.; Hess, B. A. *J. Chem. Phys.* **2003**, *118*, 7215–7225.

(51) Boese, A. D.; Klopper, W.; Martin, J. M. L. *Int. J. Quant. Chem.* **2005**, *104*, 830–845.

(52) Boese, A. D.; Klopper, W.; Martin, J. M. L. *Mol. Phys.* **2005**, *103*, 863–876.

(53) Becke, A. D. *Phys. Rev. A* **1988**, *38*, 3098–3100.

(54) Perdew, J. P. *Phys. Rev. B* **1986**, *33*, 8822–8824.

(55) Hay, P. J.; Wadt, W. R. *J. Chem. Phys.* **1985**, *82*, 270–283.

(56) Shao, Y.; Molnar, L.; Jung, Y.; Kussmann, J.; Ochsenfeld, C.; Brown, S.; Gilbert, A.; Slipchenko, L.; Levchenko, S.; O'Neill, D.; DiStasio, R.; Lochan, R.; Wang, T.; Beran, G.; Besley, N.; Herbert, J.; Lin, C.; Van Voorhis, T.; Chien, S.; Sodt, A.; Steele, R.; Rassolov, V.; Maslen, P.; Korambath, P.; Adamson, R.; Austin, B.; Baker, J.; Byrd, E.; Dachsel, H.; Doerksen, R.; Dreuw, A.; Dunietz, B.; Dutoi, A.; Furlani, T.; Gwaltney, S.; Heyden, A.; Hirata, S.; Hsu, C.; Kedziora, G.; Khalliulin, R.; Klunzinger, P.; Lee, A.; Lee, M.; Liang, W.; Lotan, I.; Nair, N.; Peters, B.; Proynov, E.; Pieniazek, P.; Rhee, Y.; Ritchie, J.; Rosta, E.; Sherrill, C.; Simmonett, A.; Subotnik, J.; Woodcock, H.; Zhang, W.; Bell, A.; Chakraborty, A.; Chipman, D.; Keil, F.; Warshel, A.; Hehre, W.; Schaefer, H.; Kong, J.; Krylov, A.; Gill, P.; Head-Gordon, M. *Phys. Chem. Chem. Phys.* **2006**, *8*, 3172–3191.

(57) Hamm, P.; Woutersen, S. *Bull. Chem. Soc. Jpn.* **2002**, *75*, 985–988.

(58) Lehoucq, R. B.; Sorensen, D. C.; Yang, C. *ARPACK: Solution of Large Scale Eigenvalue Problems by Implicitely Restarted Arnoldi Methods*; Department of Mathematical Sciences, Rice University: Houston, TX, 1997. http://www.netlib.org/scalapack/index.html.

(59) Boese, A. D.; Martin, J. M. L. *J. Phys. Chem. A* **2004**, *108*, 3085–3096.

(60) Adams, D. M.; Hooper, M. A.; Squire, A. *J. Chem. Soc. A* **1971**, 71–77.

(61) Nee, M.; Baiz, C.; Anna, J.; McCanne, R.; Kubarych, K. *J. Chem. Phys.* **2008**, *129*, 084503.

(62) Baiz, C. R.; McRobbie, P. L.; Anna, J.; Geva, E.; Kubarych, K. J. *J. Phys. Chem. A*, **2009**, *113* (31), pp 8907–8916.

(63) Baiz, C.; Nee, M.; McCanne, R.; Kubarych, K. *Opt. Lett.* **2008**, *33*, 2533–2535.

(64) Zhuang, W.; Abramavicius, D.; Hayashi, T.; Mukamel, S. *J. Phys. Chem. B* **2006**, *110*, 3362–3374.

(65) Naraharisetty, S. R. G.; Kasyanenko, V. M.; Rubtsov, I. V. *J. Chem. Phys.* **2008**, 128.

(66) Kurochkin, D. V.; Naraharisetty, S. R. G.; Rubtsov, I. V. *Proc. Natl. Acad. Sci. U.S.A.* **2007**, *104*, 14209–14214.

(67) Ding, F.; Zanni, M. T. *Chem. Phys.* **2007**, *341*, 95–105.

(68) Bredenbeck, J.; Helbing, J.; Hamm, P. *J. Am. Chem. Soc.* **2004**, *126*, 990–991.